Mathematical Model of Parabolic Trough Collector with Fresnel Lens as Second Collector

Abdullah Aljarwi, Adnan K. Al-Salihi[1]& F. Yehay[2*]
[1]Department of mathematical, Education faculty, Albaydha University, Albaydha, Yemen
[2]Department of Physics, Education band Sciences faculty, Albaydha University, Albaydha, Yemen
*fahembajash@gmail.com

DOI: https://doi.org/10.56807/buj.v6i1.563

Abstract

Parabolic trough collectors (PTCs) have came out as a promising technology for harnessing solar energy for various applications including electricity generation and thermal heating. However, improving their thermal performance remains a critical challenge to maximize energy conversion efficiency. This paper presents a mathematical model for enhancing the thermal performance of PTCs by using a curved Fresnel lens as a second collector over the top side of the receiver. This enhancing has taken advantage of the space above the top side of receiver and increased the thermal efficiency of PTCs. The unsteady heat transfer equations with one dimension are used to simulate the effect of Fresnel lens on the receiver components beside the heat transfer fluid and compared with that without Fresnel lens. The results of this model are based on parameters of LS-2 model and environment of installation place whereas the water was chosen as heat transfer fluid with physical properties depending on Temperature. Al-Baydha city in Yemen is chosen as an installation place taking in consideration the variation of environment temperature in each month of the year and the inlet temperature of water and receiver's components are taken as the minimum temperature of the air.

***Keywords**: Mathematical Model; Parabolic Trough Collector; Fresnel Lens ; Solar*

النموذج الرياضي للمجمع ذو القطع المكافئ مع عدسة فريسنل كمجمع ثانٍ

عبدالله الجروي، عدنان الصالحي، فاهم بجاش
جامعة البيضاء

ملخص

لقد ظهرت مجمعات الحوض المكافئ (PTCs) كتقنية واعدة لتسخير الطاقة الشمسية لمختلف التطبيقات بما في ذلك توليد الكهرباء والتدفئة الحرارية. ومع ذلك، فإن تحسين أدائها الحراري يظل تحديًا كبيرًا لتحقيق أقصى قدر من كفاءة تحويل الطاقة. يعرض هذا البحث نموذجًا رياضيًا لتعزيز الأداء الحراري لـ PTCs باستخدام عدسة فريسنل المنحنية كمجمع ثانٍ فوق الجانب العلوي من جهاز الاستقبال. استفاد هذا التحسين من المساحة الموجودة أعلى الجانب العلوي لجهاز الاستقبال وزاد من الكفاءة الحرارية لـ PTCs.تم استخدام معادلات انتقال الحرارة غير المستقرة ذات البعد الواحد لمحاكاة تأثير عدسة فريسنل على مكونات المستقبل بجانب مائع نقل الحرارة ومقارنتها مع تلك التي لا تحتوي على عدسة فريسنل. نتائج هذا النموذج تعتمد على معايير نموذج LS-2 وبيئة مكان التركيب حيث تم اختيار الماء كسائل ناقل للحرارة ذو خواص فيزيائية تعتمد على درجة الحرارة. تم اختيار مدينة البيضاء في اليمن كمكان للتركيب مع الأخذ في الاعتبار اختلاف درجة حرارة البيئة في كل شهر من أشهر السنة، كما تؤخذ درجة حرارة مدخل الماء ومكونات جهاز الاستقبال كأدنى درجة حرارة للهواء.

الكلمات المفتاحية: النموذج الرياضي؛ جامع الحوض المكافئ؛ عدسة فريسنل ؛ شمسي

1. Introduction

The solar energy is the one of main, cleanest and most sustainable forms of energy available to use in many industrial applications today. Therefore there are many of techniques to benefit of this power. The concentered collectors are one of these techniques. Parabolic trough collectors (PTCs) are one of the concentrated collectors technologies and are widely used in solar thermal power plants to harness solar energy for electricity generation and other industrial applications of medium and high-temperature levels. Parabolic trough collectors are the most mature concentrating collectors because they have real applications and are the most commercially and technically developed. Solar Electric Generating Systems (SEGS) plants were the biggest commercial plants of PTCs, they have been built by Luz International and installed in California's Majove Desert, SEGS-I was the first plant with capacity 14-MW electric (MWe) and amplified by adding SEGS-II until SEGS-IX, SEGS plants have total capacity of 354MWe) Duffie et al. (2020); Coccia et al. (2016). These plants were the first plants and they have been in successful operations since early 1980's Mwesigye et al. (2012).

The collectors which have been designed for these plants are LS-1 for SEGS-I, LS-2 for SEGS-II to SEGS-VII and LS-3 for a part of SEGS-VII to SEGS-IX plant Duffie et al. (2020).

Basically, PTC consists of curved mirrors, generally in a parabolic shape, which concentrate sunlight onto a receiver tube located along the focal line. The receiver tube contains a heat transfer fluid that absorbs the concentrated solar energy and transfers it to a power cycle or heat exchanger. While parabolic trough collectors have shown great potential, there are still challenges that need to be addressed such as heat losses, cost reduction, tube absorber design, accuracy of tracking system,...etc. In recent years, there has been a growing focus on enhancing the performance and efficiency of PTCs by using various methods. This includes enhancing the materials of heat-absorbing for better heat transfer and thermal energy storage, improving tracking systems for increasing the amount of solar energy collected which improve their optical design and maximize sunlight capture, and optimizing the overall system to minimize heat losses and increase the overall energy conversion efficiency. Enhancements in receiver technology and heat transfer fluid play a significant role in improving the overall performance of PTCs.

Many of researches have focused on developing high-performance absorber coatings, numerically and experimentally comparing among heat transfer fluids, and novel receiver designs to enhance thermal efficiency, reduce heat losses, and increase temperature capabilities. Inserting types in absorber tube such as fins, coils, spiral grooved, … etc. The inserting types have been studied by many researches to enhance heat transfer coefficient for increasing thermal performances. Here some of researches that focused on inserts types. Inserted a type called a twisted type with wall-detached inside absorber tube was increased thermal efficiency by about 10 % at a twist ratio of greater than one due to presence of twisted tapes and the entropy generation had greatest reduction about 58.8% Mwesigye et al. (2016).

Inserting Metal foam in absorber tube was examined by Jamal-Abad et al. (2017) who found that thermal efficiency increased up to 3% Nusselt number increased 8 times and the extremely high pressure drop increased over 100 times.

The enhancing solar power technology is considered one of the most subjects which many of researches focus on.

2. The Second Collector

The idea of using a second collector is not new, where Bellos and Tzivanidis (2019) showed different types of second collector and enhanced methods. However in this paper the use of curved Fresnel lens as a second collector for parabolic trough collector is presented. Where, the top part of the receiver of parabolic trough collector was covered by curved Fresnel lens ensure receiving the absorber tube high solar radiation density at top side as seen in figure 1.

Fresnel lenses are widely used in many application especially in solar concentrating system, they have especial advantage to other lenses such as small volume, mass production, low cost and light weight as well as effectively increase of the energy density. Fresnel lens can be made of glass and plastics materials that have optical specifications similar to glass such as polymethylmethacrylate (PMMA), acrylic and polycarbonate Xie et al. (2013). Therefore, Fresnel lenses offer high optical efficiency when they were used as solar concentrators with minimal weight and cost.

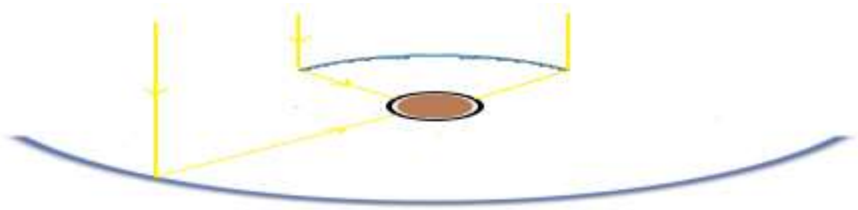

Figure 1: Cross section of purpose model

3.1. Mathematical Model

The mathematical model bases on energy balance of the receiver's components with using the Fresnel lens as second concentrator beside the parabolic concentrator to explain how Fresnel lens has effect on the performance of parabolic trough collector. This model is basing a assumption which used to build this pattern, neglecting the heat distribution from the top to bottom or vice versa of absorber sides by variation of temperature.

3.1.1 Concentration ratio of Fresnel lens

The concentration ratio of Fresnel lens is given by Xie et al. (2013)

$$C_f = \frac{A_f}{A_r} \qquad (1)$$

Where A_f is the aperture area of Fresnel lens and A_r is the area of receiver that facing the Fresnel lens. Since the receiver and the lens have the same length then the concentration ratio can be given as

$$C_f = \frac{S_f}{S_r} \qquad (2)$$

Where S_f is arc of the Fresnel lens and S_r is arc of the receiver, Which they are

$$S_f = R_f(2\theta \times \frac{\pi}{180}) \qquad (3)$$

$$S_r = r_c(2\theta \times \frac{\pi}{180}) \qquad (4)$$

r_c is the radius of receiver and R_f is the radius of the lens which is evaluated from figure 2 by

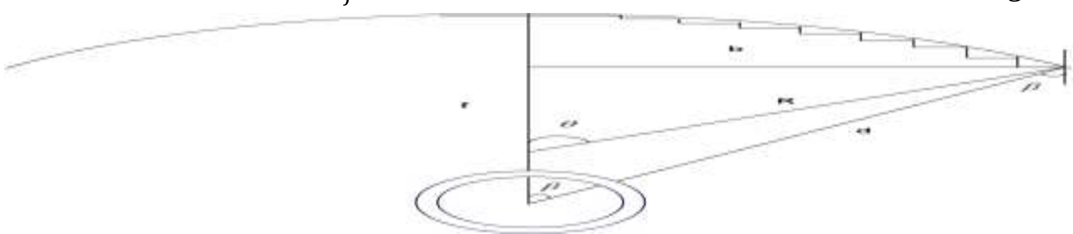

Figure 2 Schematic diagram of a half line-focus curved Fresnel lens

$$R_f = \frac{b}{\sin(\theta)} \tag{5}$$

And the focal f length is given as

$$f = \frac{b}{\tan(\beta)} + R_f - \sqrt{{R_f}^2 + b^2} \tag{6}$$

Where β is the angle between the focal line and the center ray as figure 2 showed. The relation between the distance from the center of receiver to a groove and the radius of the receiver is in equation 7, this equation can be using for restricting of refraction rays losses Xie et al. (2013)

$$d \leq \frac{r_c}{2\tan(\xi)} \tag{7}$$

Where ξ is the half angle between the sun and the earth, which is 0.27◦ and d is given from figure 2 as

$$d \approx \sqrt{b^2 + (f - R_f + \sqrt{{R_f}^2 - b^2})^2} \tag{8}$$

From figure 3, we see that since the size of the grooves are very small then the slope angle of a groove and the arc of groove can be approximated as

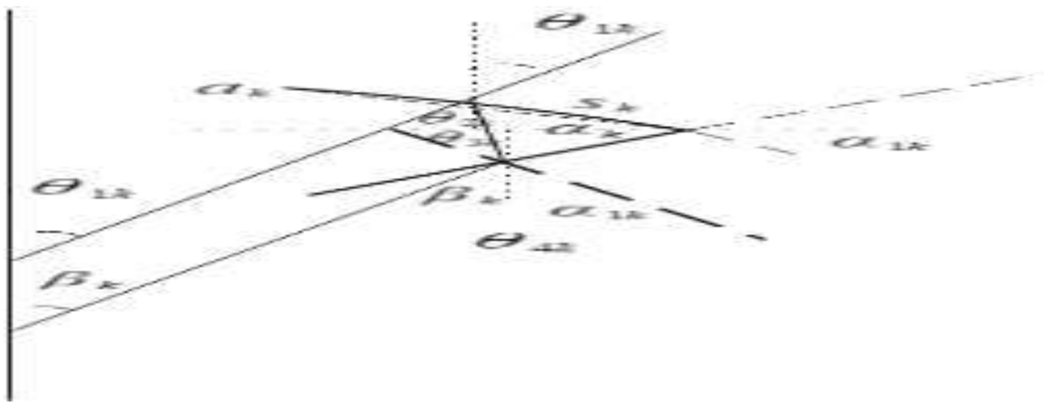

Figure 1: A groove geometry

$$a_k \approx S_k \tag{9}$$

And

$$\alpha_k \approx \theta_{2k} + \theta_{3k} \tag{10}$$

Then

$$a_k \approx R\,\theta_{1k} \tag{11}$$

Let x_i is the width of the prism, Then

$$x_i = a_k \cos(\alpha_k) \tag{12}$$

If all prisms have the same width and their number are m , then

$$x_i = \frac{b}{\mathrm{m}} \tag{13}$$

From Snell's low refraction, we have

$$\sin(\theta_{1k}) = n \sin(\theta_{2k})$$
$$\sin(\theta_{4k}) = n \sin(\theta_{3k})$$

Where n is the refractive index of lens material. By considering that, The lens is fastened to receiver which is tracked, then incident angle should be small. If the incidence angle is 0° then from figure we have

$$\alpha_k \approx \Theta_{1k} + \Theta_{4k} - \beta_k$$

Where k indicates the number of the groove, $\theta_{1k}$is the angle between the end radius of that groove, θ_{4k} is refractive angle of the ray that leaves the prism to focal point and β_k is the angle between focal length and the refractive ray. Therefore,

$$\theta = \sum_{k=1}^{m} \theta_{1k}$$

$$\beta = \sum_{k=1}^{m} \beta_k$$

To evaluate the concentrating solar energy intensity on the receiver (G_r) by Fresnel lens that hits the absorber, we can use the following equation.

$$G_r = \eta_f I_b C_f \tag{14}$$

Where I_b is the direct solar radiation and η_f is the optical efficiency of Fresnel lens that depends on the incident angle in addition to many parameters. the optical efficiency is defined by

$$\eta_f = \frac{\text{absorbed energy by the receiver}}{\text{incicdent energy on the outer surface of lens}}$$

The energy absorbed by receiver from the Fresnel lens is given by

$$Q_f = \eta_f I_b A_f \tag{15}$$

The total energy absorbed by the receiver from both the Fresnel lens and parabolic trough collector can be given by the equation

$$Q_{ab} = Q_f + Q_{co} \tag{16}$$

Where Q_{co} is the energy absorbed by the receiver from parabolic trough collector which is given as

$$Q_{co} = \eta_c I_b A_c \tag{17}$$

Where η_c is the optical efficiency of parabolic trough collector, A_c is the trough collector area (m^2).

3. Thermal Model

Thermal model bases on the analysis of heat behavior of the receiver's components with effect of the curved line Fresnel lens beside parabolic trough collector as concentrating surfaces.

4.1. The heat transfer in glass envelope

The heat transfer equation per unit length of the glass cover of the absorber tube of PTCs in one dimension with constant physical properties is given by

$$A_g C_{Pg} \rho_g \frac{\partial T_g}{\partial t} = A_g k_g \frac{\partial^2 T_g}{\partial x^2} + Q_{ab}^{g} + Q_{gin_{a-g}} - Q_{los_{g-air}} \tag{18}$$

Where A_g, C_{Pg}, ρ_g and k_g are the cross-area (m^2), specific heat at constant pressure(J/kg K), density (kg/m^3) and thermal conductivity (J/m K) of the glass envelop respectively. Q_{ab}^{f} is the absorbed energy by glass envelope from solar radiation (W/m) and $Q_{gin_{a-g}}$, $Q_{los_{g-air}}$ are gain energies from absorber tube and losses energies from glass cover to environment (W/m). Where

$$Q_{ab}^{f} = \alpha_g Q_{ab} \tag{19}$$

Where α_g is the absorptance factor of glass. And

$$Q_{gin_{a-g}} = Q_{c_{a-g}} + Q_{r_{a-g}} \tag{20}$$

$Q_{c_{a-g}}$ and $Q_{r_{a-g}}$ are the energies lost from absorber into glass cover by convection and radiation respectively. The convection heat transfer in annulus and mainly depending on the pressure in annulus, where at pressure less than (1torr), the collisions seldom occur between molecules of gas in annulus, therefore the heat transmits by free-molecular convection Xu et al. (2019); Yunus A. Çengel (2015). The recommended pressure to neglect the loss by convection is under vacuum (0.013Pa) or near this region Padilla et al. (2011). In general the energy losses per unit length by convection over horizontal cylinder is given by Newton cooling law as

$$Q_{c_{a-g}} = \pi D_{a_{ex}} h_{c_{a-g}} (T_a - T_g) \tag{21}$$

Where $D_{a_{ex}}$ is the outer diameter of the absorber tube (m), $h_{c_{a-g}}$ is a convection heat transfer coefficient(W/m^2K). T_a, T_g are temperatures of the absorber and glass cover respectively (◦C). A correlation of $h_{c_{a-g}}$ for annulus gas under vacuum is given by Xu et al. (2019)

$$h_{c_{a-g}} = k_{std} \left[\frac{D_{a_{ex}}}{2} \ln\left(D_{ag}^*\right) + \frac{(9\vartheta - 5)\left(D_{ag}^* + 1\right)\lambda_m}{2(\vartheta + 1)} \right]^{-1} \tag{22}$$

Where k_{std} is the thermal conductivity at standard temperature and pressure D_{ag}^* is the ratio between the inner diameter of the glass to outer diameter of the absorber. ϑ is the ratio between the specific heat of gas in annulus at constant pressure to that at constant volume. λ_m is mean-free-path between collisions of the molecule (m) and given Xu et al. (2019) as

$$\lambda_m = \frac{B\bar{T}_{ag}}{\pi\sqrt{2}P_n D_m^2} \tag{23}$$

here B is Boltzmann's constant (1.381×10−23 (J/K)), P_n is the pressure in annulus (Pa). D_m is molecular diameter of annulus gas (m). Table 1 gives the coefficients of heat transfer for common annulus gases. If the vacuum in annulus is lost, the heat transfer between the absorber and glass cover occurs by natural convection. The correlation of convection heat transfer coefficient for natural convection is Yunus A. Çengel (2015) by

$$h_{c_{a-g}} = \frac{k_{eff}}{D_{a_{ex}} \ln\left(D_{ag}^*\right)} \tag{24}$$

Where k_{eff} is the effective thermal conductivity and given by

Table 1: Coefficients of heat transfer for common annulus gases Xu et al. (2019); Forristall (2003)

Gas	k_{std} (W/m K)	D_m $(10^{-10}\ m)$	ϑ
Air	0.02551	3.72	1.4034
Hydrogen	09090	2.74	1.408
Argon	0.01777	3.8	1.677

$$k_{eff} = 0.386 k_{std} \left[\frac{Pr_{gs}}{0.861 + Pr_{gs}} \right]^{\frac{1}{4}} \left(F_g Ra_{gs}\right)^{\frac{1}{4}} \tag{25}$$

Where F_g is the geometric factor for concentric cylinders. Pr_{gs} is the Prandtl number for gas properties and Rags is the Rayleigh number and they are evaluated at the average temperature of the outer surface of absorber and the inner surface of glass ($\bar{T}_{ag}$). This correlation is suitable in the range (Ra ≤ 107) and (0.7 ≤ Pr ≤ 6000). In addition to that, for the case when k_{eff} is less than k_{std}, the k_{eff}

should be replaced by k_{std} Xu et al. (2019); Yunus A. Çengel (2015). Where F_g , $Ra_{gs}$and Pr_{gs} are given by

$$F_g = \frac{\ln\left(D_{ag}^*\right)^4}{L_{ch}^3 (D_{a_{ex}}^{-0.6} + D_{g_{in}}^{-0.6})^5} \tag{26}$$

L_{ch} is the characteristic length (m) for Rayleigh number and is given by

$$L_{ch} = \frac{D_{g_{in}} - D_{a_{ex}}}{2}$$

Rayleigh number is given by

$$Ra_{avg} = \frac{g\Upsilon(T_a - T_g)L_{ch}^3}{\alpha_{d_{avg}} \nu_{avg}} \tag{27}$$

Where g is gravity acceleration (9.8 (m/s2)). Υ is thermal expansion coefficient (1/K) which is

$$\Upsilon = \frac{1}{T + 273.15}$$

ν_{avg} is kinematic viscosity (m^2/s). $\alpha_{d_{avg}}$ is thermal diffusivity (m^2s). The Prandtl number for gas is given by

$$Pr_{gs} = \frac{C_{P_{gs}} \mu_{gs}}{k_{gs}}$$

Where μ_{gs} is dynamic viscosity (kg/m s). k_{gs} is thermal conductivity of gas.

The energy lost per unit length by radiation from the outer surface of the absorber to the envelope glass is

$$Q_{r_{a-g}} = \pi D_{a_{ex}} h_{r_{a-g}} (T_a - T_g) \tag{28}$$

Where $h_{r_{a-g}}$ the coefficient of heat transfer by radiation Xu et al. (2019) and is

$$h_{r_{a-g}} = \frac{\sigma((T_a + 273.15)^2 + \left(T_g + 273.15\right)^2)(T_a + T_g + 546)}{\frac{1}{\epsilon_a} + \frac{(1-\epsilon_g)}{D_{ag}^* \,\epsilon_g}} \tag{29}$$

Where ϵ_g and ϵ_a are the emissivity of the glass cover and the absorber in the long-wavelength range.

4.2. The heat transfer in the absorber tube

The reflected solar radiation from parabolic collector into the absorber tube that absorbs the most of this energy and transmits it into HTF by convection. The other energy losses into glass cover and tips. The mechanisms of heat transfer into and from the absorber is given by first thermodynamics law with taken some considerations in the model. The physical properties of the absorber is considered constants and the energy lost by conduction either between the absorber and glass cover or at the ends of absorber are negligible. The energy balance equation in one dimension of absorber tube per unit length is given as

$$A_a C_{Pa} \rho_a \frac{\partial T_a}{\partial t} = A_a k_a \frac{\partial^2 T_a}{\partial x^2} + Q_{ab}^a - Q_{gin_{a-g}} - Q_{c_{a-f}} \tag{30}$$

A_a is the cross-section area of absorber (m^2). Q_{ab}^a is the absorbed energy by the absorber (W/m). $Q_{c_{a-f}}$ is the energy lost from the inner surface of absorber by convection which is evaluated by Newton cooling law. Therefore the energy lost by convection per unit length from the inner surface of absorber and the heat transfer flow is

$$Q_{c_{a-f}} = \pi D_{a_{in}} h_{c_{a-f}} (T_a - T_f) \tag{31}$$

Where $D_{a_{in}}$ is the inner diameter of absorber (m). T_f is the temperature of the heat transfer fluid stream. The convection heat transfer coefficient for the fluid is evaluated by

$$h_{c_{a-f}} = \frac{Nu_f k_f}{D_{a_{in}}} \tag{33}$$

Nu_f is Nusselt number which in general is a function of Prandtl number and Reynolds number (Re), then it depends on the geometry of the flow beside on the fluid properties. The correlation for Nusselt number which can be used for flow through tube is given by Meyer et al.(2019)

$$Nu_f = (Nu_{lm}^{10} + (Nu_{tu}^{-8} + Nu_{tr}^{-8})^{\frac{-10}{8}})^{\frac{1}{10}} \tag{34}$$

Where Nu_{lm} , Nu_{tu} and Nu_{tr} are Nusselt numbers for laminar, turbulent and transitional flow regions respectively. For laminar region when $Re \leq 2300$, the Nusselt number is

$$N_{lm} = 4.36 + \frac{1}{L}\,(Nu_1 + Nu_2) \tag{35}$$

Where

$$Nu_1 = -0.84Pr^{-0.2}L_t + 0.72\,(ReD_{a_{in}})^{0.54}Pr^{0.34}L_t^{0.46} \tag{36}$$

$$Nu_2 = (0.207Gr^{0.305} - 1.19)Pr^{0.42}\left(ReD_{a_{in}}\right)^{-0.08}(L - L_t) \tag{37}$$

Where

$$L_t = min\left\{\frac{2.4RePr^{0.6}D_{a_{in}}}{Gr^{0.57}}, L\right\}$$

The hydraulic diameter can used instead of $D_{a_{in}}$ for accurate Karwa.(2017). For turbulent flow, the Nusselt number correlation is

$$Nu_{tu} = 0.18Re^{-0.25}(Re - 500)^{1.07}Pr^{0.42}\left(\frac{Pr}{Pr_s}\right)^{-0.08} \tag{38}$$

For transitional flow regime

$$Nu_{tr} = (0.017Re - 30.3)Pr^{0.33}\,Gr^{-0.08} \tag{39}$$

Where Re, Pr and Gr are Reynolds, Prandtl and Grashof numbers and they are evaluated by

$$Re = \frac{4\dot{m}}{\pi D_{a_{in}}\mu_f}$$

$\dot{m}$ is mass flow rate (kg/s)

$$Pr = \frac{C_{P_f}\mu_f}{k_f}$$

$$Gr = g\Upsilon D_{a_{in}}^3(T_{f_{avg}} - T_b)\left(\frac{\rho_f}{\mu_f}\right)^2$$

Where T_b and $T_{f_{avg}}$ are bulk temperature and the average temperature of the fluid, where

$$T_b = \frac{T_f + T_a}{2}$$

$$T_{f_{avg}} = \frac{1}{L}\int_0^L T_f\,dx$$

4.3. The heat transfer in water

The energy balance equation of fluid in one dimension is given as

$$A_f E(T_f)\frac{\partial T_f}{\partial t} = \frac{\partial}{\partial x}\left(A_f k_f \frac{\partial T_f}{\partial x}\right) - \dot{m}C_{P_f}\frac{\partial T_f}{\partial x} + Q_{c_{a-f}} \qquad (40)$$

Where

$$E(T_f) = \frac{\partial}{\partial T_f}(T_f C_{P_f}\rho_f)$$

The physical properties of water is given by Marif et al. (2014)

$$C_{P_f} = 0.01378T_f^2 - 1.42026T_f + 4218.2371 \qquad (41)$$

$$k_f = -5.96341 \times 10^{-6}T_f^2 + 1.63 \times 10^{-3}\, T_f + 0.56821 \qquad (42)$$

$$\rho_f = -4.95626 \times 10^{-4}T_f^2 - 0.23291T_f + 1001.83736 \qquad (43)$$

$$\mu_f = -4.28265 \times 10^{-10}T_f^3 + 1.88979 \times 10^{-7}T_f^2 - 2.77774 \times 10^{-5}\, T_f + 15.610^{-10} \qquad (44)$$

4. Solar Radiation

There are many models which can be used to evaluate the Direct solar radiation on any installed location. One of those is given here. The direct solar radiation on a collector surface can be evaluated Marif et al. (2014); Othman et al. (2018) by

$$I_{dn} = E_d \cos(\Theta_i)e^{(-\delta_R T_L M_p)} \qquad (45)$$

Where E_d is the extraterrestrial radiation incident on the plane normal to the radiation on a day of the year, δ_R is the optical thickness of Rayleigh, M_p is the relative optical of mass, T_L is the Linke turbidity factor and Θ_i is incident angle of solar radiation. Where

$$E_d = 1367\left(1 + 0.00334\ \cos\left(\frac{360d}{365}\right)\right) \qquad (45)$$

d is a day number.

$$\delta_R = \frac{1}{0.9M_b + 9.4} \qquad (46)$$

$$M_b = \frac{P_{atm}}{101325\sin(\alpha_s) + 15198.75(3.885 + \alpha_s)^{-1.253}} \qquad (47)$$

Where P_{atm} is the atmospheric pressure at any location on earth surface and is given by

$$P_{atm} = 101325(1 - 2.26 \times 10^5 \times Z)^{5.25} \qquad (48)$$

Z is the altitude in meters. α_s is the solar altitude angle which is Duffie et al. (2020)

$$\alpha_s = sin^{-1}(\sin(\varphi)\sin(\delta_d) + \cos(\varphi)\cos(\delta_d)\cos(\omega)) \qquad (49)$$

φ, δ_d and δ_d are Latitude, declination and hour angle respectively. Where

$$\delta_d = 23.45\, sin\left(\frac{360(284 + d)}{365}\right) \qquad (50)$$

$$\omega = (T_{sol} - 12)15^{\circ} \qquad (51)$$

Where T_{sol} is the solar time in minutes and given by

$$T_{sol} = t_{loc} + 4(L_{st} - L_{loc}) + Eot \qquad (52)$$

L_{st} and L_{loc} are the standard meridian for the local time zone and the longitude of the location respectively. Eot is the equation of time (in minutes) where

$$Eot = 0.01719 + 0.4281456\text{cosD} - 7.3520484\text{sinD} - 3.349758\text{cos2D} - 9.371988\text{sin2D}$$

Where

$$D = \frac{(d - 1)360}{365}$$

The sunrise (ω_r) and the sunset (ω_s) angle are given by

$$\omega_r = cos^{-1}(-\,tan(\varphi) * tan(\delta_d))$$
$$\omega_s = -cos^{-1}(-\,tan(\varphi) * tan(\delta_d))$$

The times of sunrise and sunset are

$$t_r = 12 - \frac{\omega_r}{15}$$
$$t_s = 12 + \frac{\omega_r}{15}$$

Linke turbidity factor *TL* is evaluated Othman et al. (2018) by

$$T_L = 2.4 + 14.6A_t + (0.4 + 0.8\,A_t)\ln(\mathcal{P}_{vap}) \quad (53)$$

Where A_t is the coefficient of atmospheric disturbance, which its value is dependent on the locations, which is given in table 2 as Where $\mathcal{P}_{vap}$ is the partial pressure of water vapor, which is the multiply average relative humidity (H_{av}) and saturated vapor pressure $\mathcal{P}_{vap}$, they are given by Othman et al. (2018)

Table 2: Value of atmospheric disturbance coefficient *At* Othman et al. (2018)

Location	Mountain	Rural	Urban	Industrial site
A_t	0.02	0.05	0.10	0.2

$$\mathcal{P}_{vap} = H_{av}P_{stv} \quad (52)$$

Where

$$H_{av} = 0.5$$
$$P_{stv} = 2.165\left(1.098 + \frac{T_{air}}{100}\right)^{8.02} \quad (53)$$

T_{air} is the temperature of air. The incident angle is between normal to collector and beam radiation, which is given in general Duffie et al. (2020) by

$$\Theta_i = cos^{-1}\big(cos(\vartheta)cos(\beta) + sin(\vartheta)sin(\beta)cos(\psi_{so} - \psi_{su})\big) \quad (54)$$
$$\vartheta = cos^{-1}\big(cos(\delta_d)cos(\varphi)cos(\omega) + sin(\varphi)sin(\delta_d)\big) \quad (55)$$

Where ϑ is the zenith angle which is the incident angle for a horizontal surface, β is the slop angle of the collector, ψ_{so} is the solar azimuth angle and ψ_{su} is the azimuth angle of a surface. All above angle in degree.

6. 6. Results and Discussion

The energy absorbed by the absorber from both the lens and parabolic collector depends on different parameters such as the radius, focal line of lens and the radius θ angle of lens in addition to the carved area of absorber that intercepts the refractive rays from the lens and the area that intercepts. The characteristics of the model taken in this paper with properties of glass and absorber, are given in table 3 Marif et al. (2014); Hachicha et al. (2013); Zhai et al. (2010). The characteristics of parabolic trough collector are that of LS-2 Hachicha et al. (2013) as table 3 showed. The characteristics of the lens chosen are focal length, its radius of the lens as 0.5 m and 0.45.

Table 3: characteristics of the parabolic trough collector Marif et al. (2014); Hachicha et al. (2013); Zhai et al. (2010).

Characteristics	**Value**
Receiver length	7.8 m
Collector width W	5 m
Glass envelop external diameter $\mathbf{D_{g_{ex}}}$	0.115 m
Glass envelop internal diameter $\mathbf{D_{g_{in}}}$	0.105 m
Absorber tube external diameter $\mathbf{D_{a_{ex}}}$	0.070 m

Absorber tube internal diameter $\mathbf{D}_{\mathbf{a}_{\mathbf{in}}}$	0.066 m
Focal length of Fresnel length $\mathbf{f}_{\mathbf{len}}$	0.50 m
Radius of Fresnel length $\mathbf{r}_{\mathbf{len}}$	0.450 m
Thermal conductivity of glass cover $\boldsymbol{k_g}$	1.2 W/mK
Thermal conductivity of absorber cover $\boldsymbol{k_a}$	54 W/mK
Specific heat of glass cover $\boldsymbol{C_{p_g}}$	1090 J/kg.K
Specific heat of absorber tube cover $\boldsymbol{C_{p_a}}$	500 J/kg.K
Glass cover density $\boldsymbol{\rho_g}$	2230 kg/m^3
Absorber tube density $\boldsymbol{\rho_a}$	8020 kg/m^3
Optical efficiency of Fresnel lens $\boldsymbol{\eta_f}$	0.7
Absorber pipe thermal absorptance $\boldsymbol{\alpha_a}$	0.906
Glass envelop thermal absorptance $\boldsymbol{\alpha_g}$	0.02
Glass envelop transmittance $\boldsymbol{\tau_g}$	0.95
Absorber tube emittance $\boldsymbol{\varepsilon_a}$	0.14
Glass envelop emittance $\boldsymbol{\varepsilon_g}$	0.86
Reflected surface reflectivity $\boldsymbol{\rho_0}$	0.93
Mass rate flow $\dot{\boldsymbol{m}}$	2 kg/s
Shape factor γ	0.92
Optical efficiency of PTCs $\boldsymbol{\eta_c}$	0.73

The equations 16 and 17 are used to calculate the energy absorbed by receiver with Fresnel lens at top of receiver and without respectively, whereas the direct solar radiation is calculated by the equation 45. The equations 18, 30 and 40 are calculated to study the thermal performance for the glass envelope, the absorber tube and the water respectively.

6.1. Model test

The model tested by comparing the results with and without lens show the effect of Fresnel lens on the thermal behavior of parabolic receiver components and characteristics of parabolic trough collector which is taken LS-2 model as in table 3. The test of the absorbed energy by the absorber tube was taken when the parabolic collector is full tracking, rotates about East-West axis and rotates about South-North axis, in addition to incidence beam radiation on the collect area in months of January, June and November to take an approach to all the year. Table 4 Estimates the incidence angle for collector rotated about single horizontal axis with continuous adjustment and full tracking.

Model of Tracking	Incidence angle
Full tracking	$\theta_i = 0$
East-West rotated axis	$\theta_i = cos^{-1}\left(\sqrt{1-\cos(\delta_d)^2\sin(\omega)^2}\right)$
North-South rotated axis	$\theta_i = cos^{-1}\left(\sqrt{\cos(\vartheta)^2-\cos(\delta_d)^2\sin(\omega)^2}\right)$

The test is taken in a city of Yemen as installation location. This city is Al-Bayda which has latitude of 14.34 , longitude of 45.39 and altitude of 2038 m. Matlab software was used to solve the model. Figure 4 shows the energy absorbed by the absorber in the middle of a day in January compared with incidence solar radiation on both the outer surface of Fresnel lens and parabolic collector, Since the Fresnel lens was connected to the collector by supposition then it take the same tracking system. Branch A of figure 4 showed the incidence beam radiation on collector with different tracking system and shows the effect of tracking model on the incidence radiation. As for branch B, it shows the absorbed energy by absorber tube by using Fresnel lens and without Fresnel lens with effect of the tracking systems on the absorbed energy.

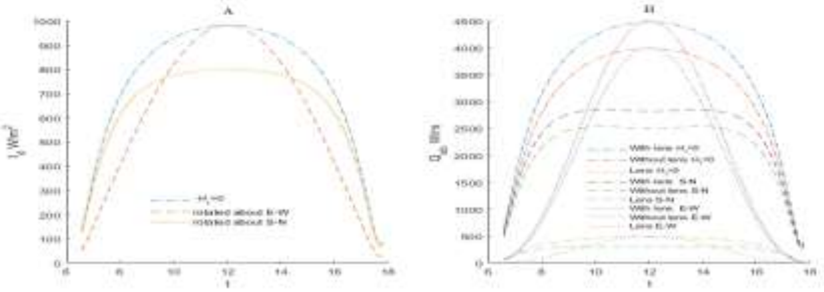

Figure 4: The energy absorbed by absorber tube compared with incidence beam radiation on collector

For full tracking system, the absorbed energy by using Fresnel lens was more increased in the maximum radiation by about 22 % than that without using Fresnel lens, for the tracking about East-West axis with continuous adjustment, the absorbed energy is the same for full tracking at the noon and for the tracking about North-South axis with continuous adjustment, the absorbed energy with using Fresnel lens was more increased in the maximum radiation by about 25% than that without using Fresnel lens.

In figure 5 Branch A showes the increased temperature of the glass envelope and the absorber tube with full tracking system at the output, the temperature of glass by using Fresnel lens is more increased in the maximum by about 12% than that without Fresnel lens in the last hour the of day and branch B shows increased temperature of the glass envelope with using Fresnel lens as a second collector and without using lens. The temperature of absorber tube by using Fresnel lens is more increased in the maximum by about 15 % than that without Fresnel lens.

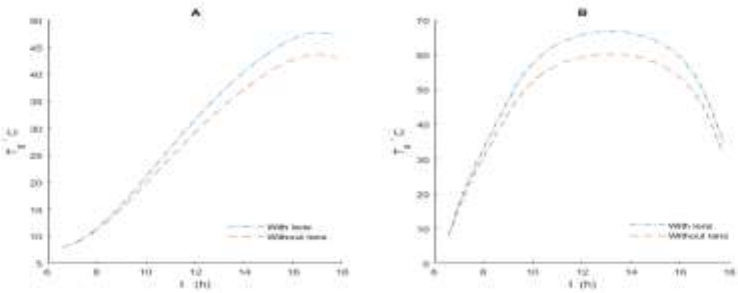

Figure 5: A - The variation of the glass envelope temperature B - The variation of the absorber tube

As for the temperature of the water, figure 6 shows the increased temperature of water by using Fresnel lens as enhancing collector with compared to without Fresnel lens with full tracking system which means the incidence angle is zero. The temperature of absorber tube by using Fresnel lens is more increased in the maximum by about 20% than that without Fresnel lens.

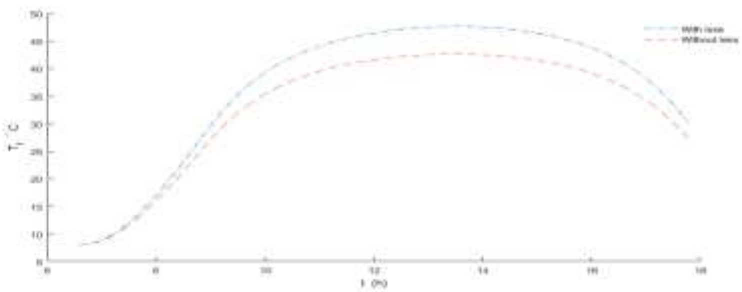

Figure 2: Temperature of water with and without lens at the output in Jan

As for the middle of the year, June month was taken to show the incidence beam radiation on the aperture area compared with energy absorbed energy by the absorber tube by using Fresnel lens and without lens as figure 7 shows also the energy absorbed by the absorber tube only from refractive radiation of Fresnel lens showed to compare all these energies. Branch A of figure 7 shows the incidence beam radiation on collector with different tracking system and shows the effect of tracking model on the incidence radiation. As for branch B, it shows the energy absorbed energy by the absorber tube by using Fresnel lens and without Fresnel lens with effect of the tracking systems on the absorbed energy. For full tracking system, the absorbed energy by using Fresnel lens was more increased in the maximum radiation by about 12 % than that without using Fresnel lens, for the tracking about North-South axis with continuous adjustment, the absorbed energy is the same as full tracking approximately and for the tracking about East-West axis with continuous adjustment, the absorbed energy with using Fresnel lens was more increased in the maximum radiation by about 12 % than that without using Fresnel lens at the noon time.

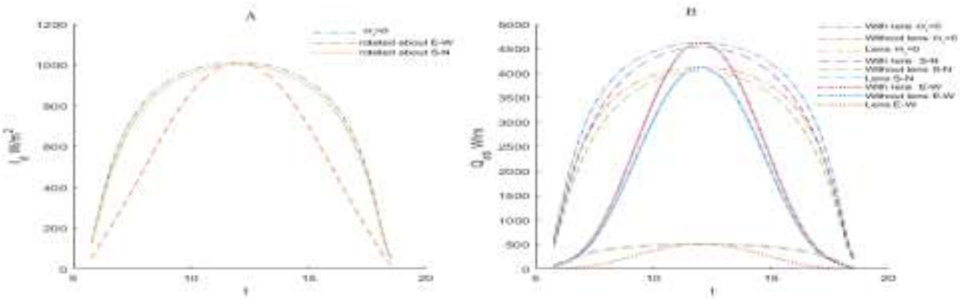

Figure 3: The energy absorbed by absorber tube compared with incidence beam radiation on collector

As for the increased temperature of the glass envelope is shown in branch A of figure 8 at the output by using Fresnel lens compared without lens with full tracking model. The temperature of glass by using Fresnel lens is more increased in the maximum by about 8% than that without Fresnel lens in the last hour of the day. Branch B shows the increased temperature of the absorber tube by using Fresnel lens and without Fresnel lens with full tracking system. The temperature of absorber tube by using Fresnel lens is more increased in the maximum by about 9% than that without Fresnel lens at the output.

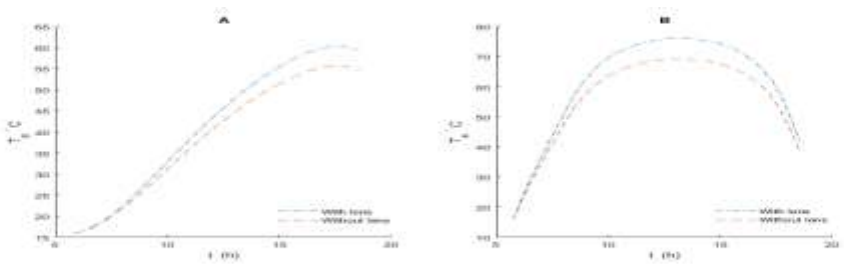

Figure 4: A - The variation of the glass envelope temperature B - The variation of the absorber tube

Increased temperature of the water, figure 9 shows the variation of water temperature by using Fresnel lens as enhancing collector compared to without Fresnel lens with the incidence angle is zero, in other word full tracking system. The temperature of water by using Fresnel lens is more increased in the maximum by about 13% than that without Fresnel lens at the output.

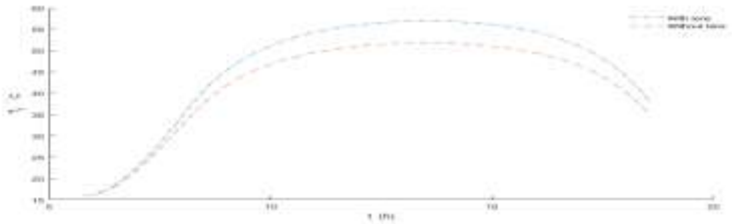

Figure 9: Temperature of water with and without lens at the output in June

At the end of the year, November month was taken to show the incidence beam radiation on the aperture area compared to the absorbed energy by the absorber tube by using Fresnel lens and without lens as figure 10 shows, Also the energy absorbed by the absorber tube only from refractive radiation of Fresnel lens shows to compare all these energies. The effect of incidence angle on the absorbed energy by using the different tracking model is shown. Branch A of figure 10 shows the incidence beam radiation on collector with different tracking system and shows the effect of tracking model on the incidence radiation. As for branch B, it shows the absorbed energy by the absorber tube by using Fresnel lens and without Fresnel lens with effect of the tracking systems on the absorbed energy. For full tracking system the absorbed energy by using Fresnel lens was more increased in the maximum radiation by about 19 % than that without using Fresnel lens, for the tracking about East-West axis with continuous adjustment, the absorbed energy is the same as full tracking at the noon time and for the tracking about North-South axis with continuous adjustment, the absorbed energy with using Fresnel lens was more increased in the maximum radiation by about 26 % than that without using Fresnel lens at the noon time.

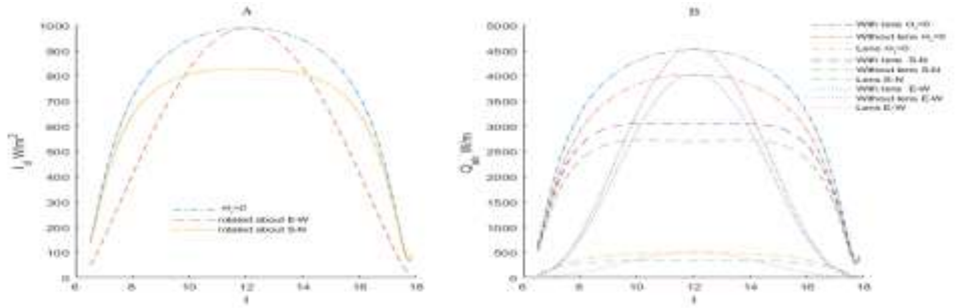

Figure 5: The energy absorbed by absorber tube compared with incidence beam radiation on collector at different tracking system in November

Increased temperature of glass envelope at the output is shown in branch A of figure 11 by using Fresnel lens compared to without lens with full tracking model. The temperature of glass by using Fresnel lens is more increased in the maximum by about 16% than that without Fresnel lens in the last hour of the day. Branch B shows the increased temperature of absorber tube by using, Fresnel lens and without Fresnel lens with full tracking system. The temperature of absorber tube by using Fresnel lens is more increased in the maximum by about 26% than that without Fresnel lens at the output.

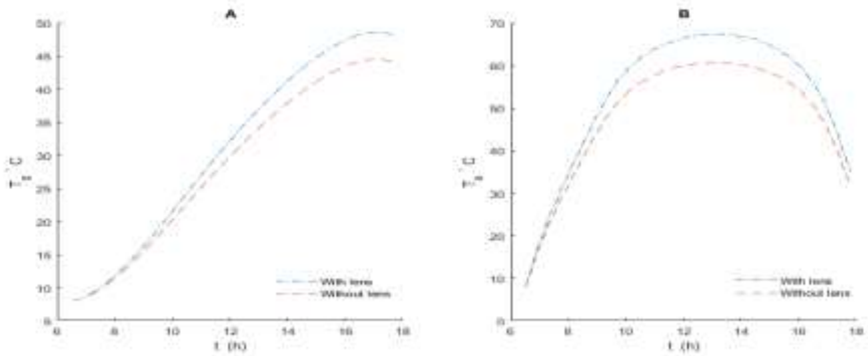

Figure 6: A - The variation of the glass envelope temperature B - The variation of the absorber tube temperature with full tracking system at the output in November

As for the temperature of the water, figure 12 shows the increased temperature of water by using Fresnel lens as an enhancing collector with compared to without Fresnel lens with full tracking system which means the incidence angle is zero. The temperature of water when using Fresnel lens is more increased in the maximum by about 11% than that without Fresnel lens at the output.

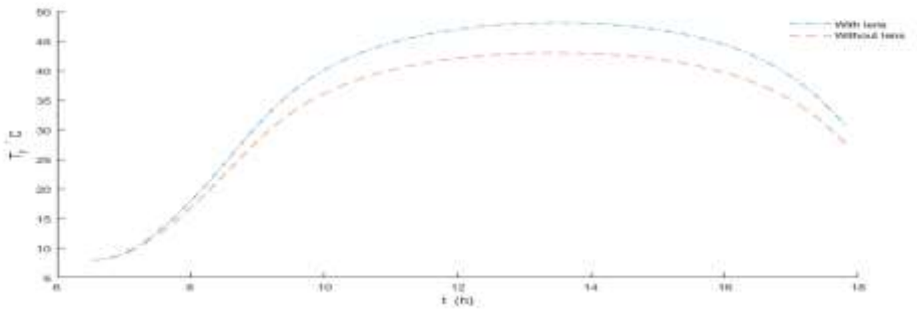

Figure 7: Temperature of water with and without lens at the output in November

In general, some months are chosan to approach all months of the year to describe the enhanced temperature using Fresnel lens. Therefore, the difference of temperature of all components of receiver with using Fresnel lens and without Fresnel lens was tested in January, June and November in middle of each month. Figure 13 shows the temperature difference of receiver components with using Fresnel lens and without Fresnel lens in middle of Jan. Branch A shows the temperature difference of receiver components with length of the absorber at the noon time and branch B shows The temperature difference of temperature through the day at the output.

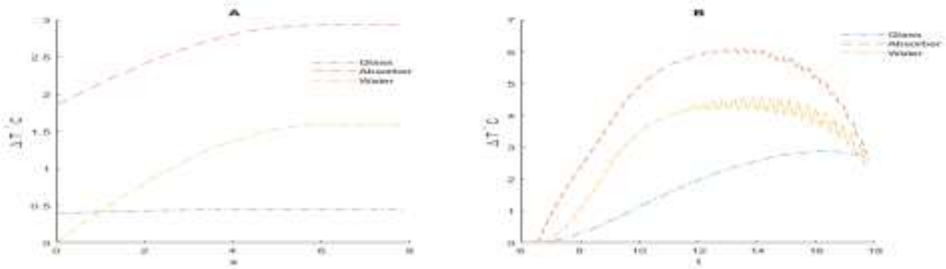

Figure 8: A -The variation of temperature along x at 12:00 B -The variation of temperature along the along the day at output in Jan

Also figure 14 shows the temperature difference of receiver components with using Fresnel lens and without Fresnel lens in middle of June .

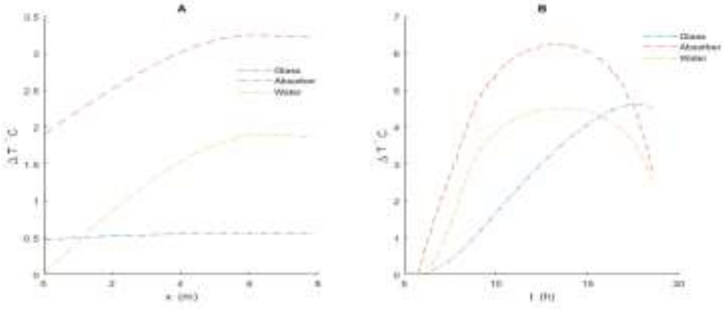

Figure 9: A -The variation of temperature along x at 12:00 B -The variation of temperature along the day in June

Also figure 15 shows the temperature difference of receiver components with using Fresnel lens and without Fresnel lens in middle of November.

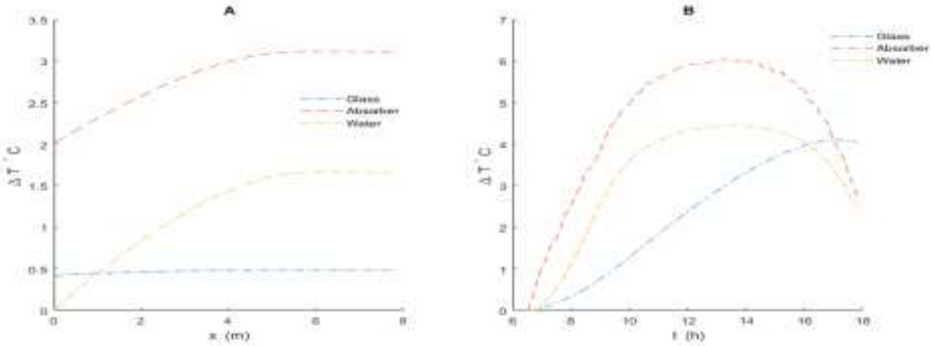

Figure 10: A -The variation of temperature along x at 12:00 B -The variation of temperature along the day in November

Table 6 gives more detail for the variation of temperature for the glass envelope, absorber tube and water with $\theta_i = 0$ at a day of each month of the year. $\bar{T}$ denotes the average temperature at output.

Table 6: Variation of temperature for glass envelope, absorber tube and water in each month by using

$\bar{T}^L$ °C	$\bar{T}^O$ °C	$\bar{T}^L_{max}$ °C	$\bar{T}^O_{max}$ °C	ΔT_{max} °C	Day	Month
			Glass envelope			
30.5993	28.3487	47.9024	43.8478	4.0546	15	Jan
33.1282	30.7001	51.4353	47.1095	4.3257	47	Feb
35.4036	32.8108	54.4093	49.8098	4.5995	75	Mar
37.9748	35.3403	57.2153	52.5510	4.6644	105	Apr
39.9421	37.2851	58.9955	54.3252	4.6703	135	May
41.7062	39.0720	60.5922	55.9482	4.6440	163	Jun
42.5685	39.9378	61.4170	56.7889	4.6281	198	Jul
41.6606	39.0280	60.7623	56.0916	4.6706	228	Aug
39.4177	36.8046	58.4812	53.8182	4.6630	258	Sep
35.5045	33.0262	54.0182	49.5864	4.4319	288	Oct
31.1982	28.9032	48.8037	44.6983	4.1054	318	Nov
29.3340	27.1012	46.3479	42.3550	3.9929	344	Dec
			Absorber tube			
53.6675	49.1332	67.5303	61.5547	5.9756	15	Jan
56.8133	52.0478	70.5809	64.3505	6.2304	47	Feb
59.1764	54.2427	72.8687	66.5253	6.3433	75	Mar

61.0430	56.1076	74.8407	68.4597	6.3810	105	Apr
61.9728	57.1212	75.8297	69.4581	6.3717	135	May
63.0302	58.2135	76.9598	70.6410	6.3188	163	Jun
64.1397	59.3329	78.0263	71.7568	6.2696	198	Jul
64.0187	59.1171	77.8396	71.5362	6.3034	228	Aug
62.5085	57.6000	76.3608	69.9176	6.4431	258	Sep
58.9287	54.0815	72.8171	66.4075	6.4096	288	Oct
54.3161	49.7188	68.1241	62.0821	6.0421	318	Nov
52.2013	47.7258	66.0383	60.1562	5.8821	344	Dec
			Water			
37.7292	34.4739	48.4816	44.0631	4.4185	15	Jan
40.3342	36.9194	51.0212	46.4672	4.5540	47	Feb
42.4007	38.8612	53.0387	48.3521	4.6866	75	Mar
44.4571	40.9389	55.0510	50.4063	4.6447	105	Apr
45.8441	42.3889	56.3861	51.7941	4.5920	135	May
47.3008	43.8777	58.0524	53.2606	4.7919	163	Jun
48.4118	45.0097	58.9160	54.4012	4.5148	198	Jul
47.9578	44.4878	58.5015	53.9117	4.5898	228	Aug
46.1715	42.6897	56.7755	52.1274	4.6481	258	Sep
42.5700	39.1005	53.5874	48.6046	4.9828	288	Oct
38.1983	34.8967	48.8860	44.4348	4.4512	318	Nov
36.3206	33.1073	47.0401	42.6747	4.3654	344	Dec

1: The temperature calculated at average at output and max denotes to maximum value at output

2 : L and O denote to Fresnel lens and without Fresnel lens

7.Conclusion

This paper attempted to discuss the effect of the curved Fresnel lens when it used as a second collector mathematically. This model tried to find a solution for the low thermal performance of PTCs especially those that have small field by adding curved Fresnel lenses to them. The effect of curved Fresnel lens on the temperatures of the receiver's components of PTCs as well as the water increased when the curved Fresnel lens was used as a second collector compared to that without Fresnel lens. The results of the model show the rising of water temperature used as heat transfer fluid. Therefore using other heat transfer fluids such as thermal oil or that with nano-technic will have more thermal efficiency. The PTCs can be enhanced by many methods which means it an open field. The results of receiver components' temperatures shows that the temperature of glass envelope has increased in an annual by about 12 % where the absorber tube had average increased in an annual by about 11% and water had average increased in an annual by about 6%˙. The optical efficiency of Fresnel lens besides geometric dimensions of the lens such as the width, radius of lens and have effect on the thermal performance . The important thing which must be taken in consideration is the effect the lens on the aperture area of parabolic trough collector to avoid the interception of solar radiation to reach the reflective mirror of PTCs. The dimensions of Fresnel lens have important effect on the heat transfer and the slope of the parabolic trough collector furthermore to tracking system which can be studied and investigated with different characteristics of Fresnel lens. The location of supposed installed place have also affect if the climate and air temperature are taken in consideration. Therefore we recommend that the behave of heat transfer of parabolic trough collector in different climates should be studied experimentally.

References

Behar, O., Khellaf, A., and Mohammedi, K. (2015). A novel parabolic trough solar collector model–validation with experimental data and comparison to engineering equation solver (ees). Energy Conversion and Management, 106:268–281.

Bellos, E. and Tzivanidis, C. (2019). Alternative designs of parabolic trough solar collectors. Progress in Energy and Combustion Science, 71:81–117. [2] A. Mwesigye, T. Bello-Ochende, J. P. Meyer, *Heat tranfer and entropy generation in a parabolic trough receiver with-detached twisted tape inserts.*, Int J Therm Sci, 99 (2016)238-257.

Coccia, G., Di Nicola, G., Hidalgo, A., et al. (2016). Parabolic trough collector prototypes for low-temperature process heat. Springer.

Duffie, J. A., Beckman, W. A., and Blair, N. (2020). Solar engineering of thermal processes, photovoltaics and wind. John Wiley & Sons.

Forristall, R. (2003). Heat transfer analysis and modeling of a parabolic trough solar receiver implemented in engineering equation solver. Technical report, National Renewable Energy Lab.(NREL), Golden, CO (United States).

Hachicha, A., Rodr´ıguez, I., Capdevila, R., and Oliva, A. (2013). Heat transfer analysis and numerical simulation of a parabolic trough solar collector. Applied energy, 111:581–592.

Jamal-Abad, M. T., Saedodin, S., and Aminy, M. (2017). Experimental investigation on a solar parabolic trough collector for absorber tube filled with porous media. Renewable Energy, 107:156–163.

Marif, Y., Benmoussa, H., Bouguettaia, H., Belhadj, M. M., and Zerrouki, M. (2014). Numerical simulation of solar parabolic trough collector performance in the algeria saharan region. Energy conversion and management, 85:521–529.

Meyer, J. P., Everts, M., Coetzee, N., Grote, K., and Steyn, M. (2019). Heat transfer coefficients of laminar, transitional, quasi-turbulent and turbulent flow in circular tubes. International Communications in Heat and Mass Transfer, 105:84–106.

Mwesigye, A., Bello-Ochende, T., and Meyer, J. P. (2012). Numerical analysis of thermal performance of an externally longitudinally finned receiver for parabolic trough solar collector. HEFAT 2012.

Mwesigye, A., Bello-Ochende, T., and Meyer, J. P. (2016). Heat transfer and entropy generation in a parabolic trough receiver with wall-detached twisted tape inserts. International Journal of Thermal Sciences, 99:238–257.

Othman, A. B., Belkilani, K., and Besbes, M. (2018). Global solar radiation on tilted surfaces in tunisia: Measurement, estimation and gained energy assessments. Energy Reports, 4:101–109.

Padilla, R. V., Demirkaya, G., Goswami, D. Y., Stefanakos, E., and Rahman, M. M. (2011). Heat transfer analysis of parabolic trough solar receiver. Applied energy, 88(12):5097–5110.

R. K. (2017). Heat and Mass Transfer. Springer Singapore.

Swinbank, W. C. (1963). Long-wave radiation from clear skies. Quarterly Journal of the Royal Meteorological Society, 89(381):339–348.

Wang, J., Wang, J., Bi, X., Wang, X., et al. (2016). Performance simulation comparison for parabolic trough solar collectors in china. International Journal of Photoenergy, 2016.

Xie, W., Dai, Y., and Wang, R. (2013). Thermal performance analysis of a line-focus fresnel lens solar collector using different cavity receivers. Solar Energy, 91:242–255.

Xu, L., Sun, F., Ma, L., Li, X., Lei, D., Yuan, G., Zhu, H., Zhang, Q., Xu, E., and Wang, Z. (2019). Analysis of optical and thermal factors' effects on the transient performance of parabolic trough solar collectors. Solar Energy, 179:195–209.

Yunus A. C¸ engel, A. J. G. (2015). Heat and mass transfer: fundamentals and applications. McGraw-Hill Education, 5 edition.

Zhai, H., Dai, Y., Wu, J., Wang, R., and Zhang, L. (2010). Experimental investigation and analysis on a concentrating solar collector using linear fresnel lens. Energy Conversion and Management, 51(1):48–55.